Conference Proceedings

EuroSun 2016
Palma de Mallorca (Spain), 11 - 14 October 2016

Modelling of a Solar Dryer for Food Preservation in Developing Countries

Joakim Olsson[1] and Henrik Davidsson[1]

[1] Lund University (Sweden)

Abstract

Food insecurity has proven to be a significant problem in many developing countries, which in some cases occurs due to the lack of adequate methods of preserving foods for longer periods of time. Solar drying of foods could be a feasible method for preserving foods in developing countries. To maintain a good product quality, the design of the solar dryer used needs to be considered. A faulty design will result in the foods being exposed to either excessive heat, which will degrade nutrients such as Vitamin C, or exposed to insufficient heat which could result in growth of mold or bacteria.

In this study a base scenario for a solar dryer design has been set up and mathematically analyzed to find ways of improving the design and identifying the most important parameters to consider. The study will serve as a part of an ongoing project at Lund University in Sweden, which will be implemented in Mozambique. The results of the study imply that the collector performance can be improved significantly if the most important parameters are optimized. For future work, more practical measurements would be required to verify the results, particularly regarding the evaporation rate of the drying products.

Keywords: *Solar drying, food preservation.*

1. Introduction

The malnutrition in developing countries has proven to be a persistent problem over the decades and appears to remain unsolved despite the economic growth that has occurred in some of the countries. Among these developing countries is Mozambique, which had a Human Development Index (HDI) positioned at rank 180 out of 188 countries and territories in 2014 by the United Nations Developing Programme, despite the HDI value being 75 % higher than in 1980 (UNDP, 2015). Almost one-third of Mozambicans, most of them living in the south and centre regions, suffer from chronic food insecurity and the country is prone and sensitive to natural disasters such as drought and flooding (World Food Programme, 2016).

Even if a major number of Mozambicans are suffering from malnutrition, it is not due to insufficient harvests. Previous studies have found that Mozambique suffer 25 % to 40 % post-harvest losses of crops, mainly due to inadequate preservation methods and infrastructure (Phinney et al., 2015). Since Mozambique currently is lacking the economical means and infrastructure to support conventional preservation methods of non-developing countries, improvement of the current drying methods is limited in terms of complexity. Having this problem in mind, an ongoing project at Lund University aims to find a simple and economical method for food preservation that can be implemented in Mozambique.

One method for preserving the fruit is using an indirect solar dryer consisting of a solar collector connected to a drying tower according to Fig. 1, which will be the main focus of this study. An indirect solar dryer uses a solar collector to heat air which is then transported to a drying unit which is protected from direct sunlight (Kumar et al., 2015). Since the sunlight doesn't directly irradiate the surface of the drying products, the risk of crust formation on the drying products, which tends to reduce the drying rate, is greatly reduced (Mills-Gray, 1994). Another benefit of an indirect solar dryer is the hygiene of the products as they are more protected from

Selection and/or peer review under responsibility of Scientific Committee
doi:10.18086/eurosun.2016.02.19 Available at http://proceedings.ises.org

the environment. To further improve the hygiene, Solar Assisted Pervaporation technology (SAP) can be used in combination with indirect solar dryers. The SAP-technology involves a textile semi-permeable to water, being impermeable to liquid water while water vapor can pass freely through the textile. Using this textile, pouches can be made to hold various fruit juices for drying, which will be referred to as SAP-pouches. The liquid fruit juice will be kept inside the pouch, protecting it from contamination, while the evaporated water can still escape the pouch. The textile is also designed to prohibit any microorganisms from entering the pouches. This means that if the fruit juice becomes pasteurized inside the pouch, it will remain sterile and thus preserve the foods for longer (Phinney et al., 2015). The drying process of indirect solar dryers mainly depends on the drying conditions inside the drying chamber, being the air mass flow rate, airflow temperature and relative humidity (Blanco-Cano et al., 2016). In other words, if these three key parameters can be improved, the dryer performance will also be improved.

The aim of the study is to set up a mathematical model for an indirect solar thermal dryer that can be used to dry SAP-pouches containing fruit juices in developing countries such as Mozambique. Furthermore, the model was used to generate simulations to identify ways of improving the dryer performance. To perform the simulations, the model was implemented in a calculation tool which could also assist the project in Mozambique in the future. The calculation tool was programmed in Maple 2015, a software used analyse, visualise and solve mathematical problems (Maplesoft, 2016).

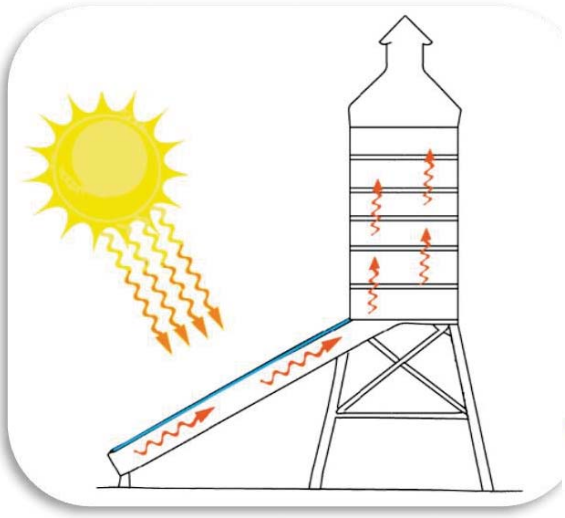

Fig. 1: Schematic figure of a solar dryer. The orange arrows inside the dryer are representing the air flow *(PAEGC & TH Cologne, 2016)*.

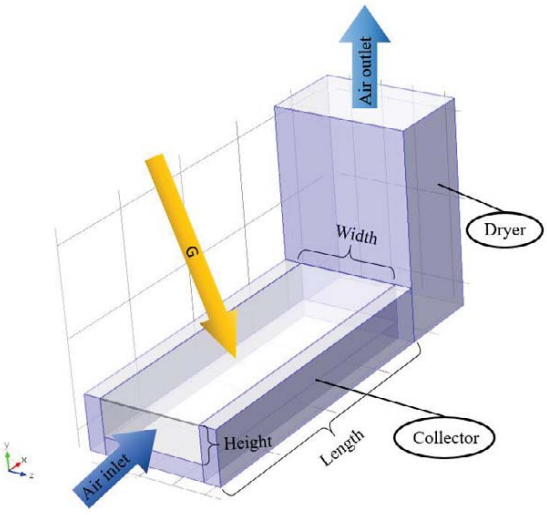

Fig. 2: Schematic figure of the model. The solar dryer is consisting of two parts: the collector and the dryer. The collector consists of a glass layer on the top, insulation on the sides and the bottom and an absorber plate on top of the bottom insulation layer. The dryer is insulated on the sides and contains shelves with SAP-pouches.

2. Method

To set up the model for the solar dryer, the solar dryer was divided into two sections according to Fig. 2; the collector and the dryer. This was essential since collector and the dryer are containing different conditions for setting up energy balances. The output air temperature of the collector will be used as an input temperature for the dryer air flow. The main idea for the model is to identify all flows of energy going in and out of the collector and the dryer in order to set up energy balances. The energy balances made for each surface of the collector and dryer respectively, i.e. the absorber plate, glazing and walls, will serve as equations that can be used in equation systems for the collector and the dryer. The equation systems are solved for relevant surface temperatures and the drying rate of the SAP-pouches is estimated from the drying conditions. To simplify the model, the following assumptions were made:

2.1. Assumptions

- The collector and dryer are in steady state for a constant solar irradiation. In reality the solar radiation will vary with time and weather conditions.
- No air leakages.
- The collector inner sides are assumed to have the mean temperature of the absorber and the glazing of the collector.
- The temperatures of the SAP-pouches are equal to the surrounding air temperature and the bags are not dried out. In practise the evaporation rate from the SAP-pouches will differ when the dryer is warming up since the pouch temperature will increase, absorbing heat.
- The parameters ρ (density), C_P (specific heat), μ (dynamic viscosity), λ_{air} (heat conductivity for air) and Pr (Prandtl number for air) have been assumed to be constant for 300 K and 1 atm.
- The inner sides of the collector will not reflect any radiation. Instead, all heat radiation is reflected between the absorber and the glass. Furthermore, the heat radiation from the absorber to the glass is also assumed to be normal to the absorber. In practise the heat will radiate in several directions from the absorber and the glass.
- Fully developed laminar air flow for Re (Reynold number) < 3000 and fully developed turbulent air flow for $3000 \leq Re \leq 5 \cdot 10^5$. For the turbulent interval, the characteristic length of the collector/dryer must be at least 10 times greater than the hydraulic diameter.
- No heat transfer between SAP-pouches.
- The ambient temperature is within the interval 0 °C < T_{amb} < 100 °C, the valid interval for using Antoine's equation for saturation pressure.
- The glass does not absorb any sunlight ($\alpha_{glass} = 0$).
- The collector sides and bottom and the dryer do not absorb any sunlight on the outside. Additional heat gains of the dryer will be added independently of the solar irradiation G.
- The convective heat transfer coefficient for all exterior walls $h_{con,\ out}$ is assumed to be a constant value of 20 W/(m²·K) (Sekhar et al., 2009) (Kumar Moningi, 2016).
- The outward heat radiation of the side areas of the collector and the dryer walls are assumed to radiate 50 % towards the sky temperature (T_{sky}) and 50 % towards the ground (T_{amb}).

2.2. The collector

For the collector, four different surfaces are identified: the glazing, the air flow, the absorber plate and the exterior walls of the sides and bottom. Each surface will have a certain temperature according to Fig. 3, dependant on the ambient conditions and the design of the collector. Energy balances for each of the four surfaces can be put together as an equation system for the entire collector and solved in Maple 2015. The energy balances will be set up with regards to the three possible ways of heat transfer; convection, conduction and radiation according to Fig. 3. Note that Fig. 3 displays the cross section of the collector and that the absorber will have absorbed some of the solar irradiation G, referred to as G_e. For explanation of all parameters used in the study, see the Nomenclature section of the appendix.

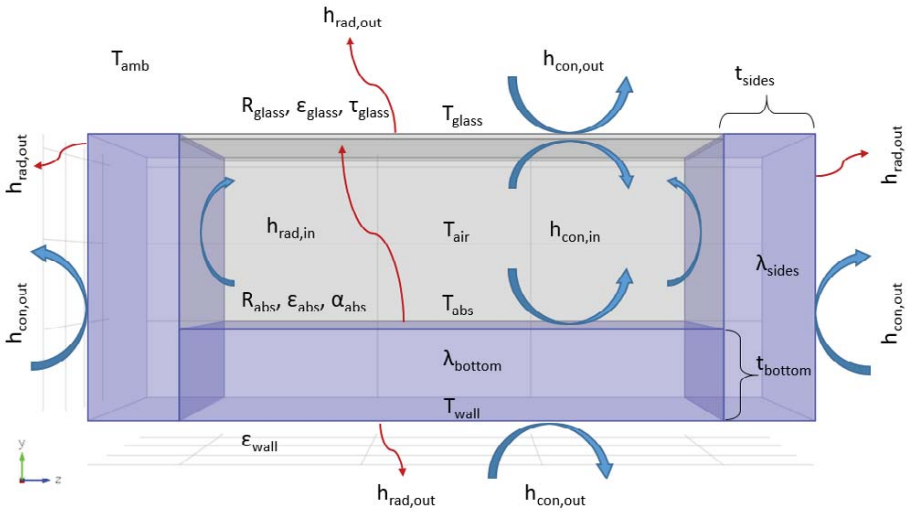

Fig. 3 : Schematic figure for all energy flows and temperatures that are included in the model for the collector. Energy balances for the glass, air flow, absorber and outer wall of the collector will be set up according to this figure. Blue arrows are representing convective heat transfer, red arrows are representing radiative heat transfer and lambdas are representing conductive heat transfer.

2.2.1 The glazing

The energy balance for the glazing consists of four energy flows according to Fig. 3. The warm absorber plate will radiate heat towards the glazing and the heated air flow will transfer heat to the glass by convection, which can be considered as the heat gains of the glazing. The heat losses of the glazing occur by radiation towards the sky and convection to the ambient air. Having identified the heat gains and losses of the glazing, the energy balance can be set up according to eq. 1.

$$h_{con,in} \cdot A_{abs} \cdot \left(\frac{T_{in}+T_{out}}{2} - T_{glass}\right) + h_{rad,in} \cdot A_{abs} \cdot \left(T_{abs} - T_{glass}\right) - h_{con,out} \cdot A_{abs} \cdot \left(T_{glass} - T_{amb}\right) - h_{rad,out} \cdot A_{abs} \cdot \left(T_{glass} - T_{sky}\right) = 0 \quad \text{(eq. 1)}$$

The external convective heat transfer coefficient $h_{con,out}$ is assumed to be a constant value of 20 W/(m²·K), but $h_{con,in}$, $h_{rad,in}$ and $h_{rad,out}$ needs to be calculated using relevant equations. Radiative heat transfer can be calculated according to eq. 2 for the heat radiating from the absorber and eq. 3 can be used to calculate the heat radiating from the glazing to the atmosphere (Incropera & Dewitt, 2002).

$$h_{rad,in} = \frac{\frac{1}{\frac{1}{\varepsilon_{abs}} + \frac{1}{\varepsilon_{glass}} - 1} \cdot \sigma \cdot \left(T_{abs}^4 - T_{glass}^4\right)}{T_{abs} - T_{glass}} \quad \text{(eq. 2)}$$

$$h_{rad,out} = \frac{\varepsilon_{glass} \cdot \sigma \cdot \left(T_{glass}^4 - T_{sky}^4\right)}{T_{glass} - T_{sky}} \quad \text{(eq. 3)}$$

The internal convective heat transfer coefficient for turbulent flows can be calculated using the definition of the Nusselt number according to eq. 4, where the definition of the hydraulic diameter of the collector can be found in eq. 5. For laminar air flows, $Re_{air} < 3000$, the Nusselt number is set to a constant value depending on the ratio between the height and the width of the collector (Incropera & Dewitt, 2002).

$$Nu = \frac{h_{con,in} \cdot D_h}{\lambda_{air}} \quad \text{(eq. 4)}$$

$$D_h = \frac{2 \cdot Height \cdot Width}{Height + Width} \quad \text{(eq. 5)}$$

To calculate the Nusselt number, eq. 6 can be used where the friction factor *f* is defined according to eq. 7. The Reynold number Re_{air} is calculated using the hydraulic diameter of the collector (Incropera & Dewitt, 2002).

$$\mathrm{Nu} = \frac{\left(\frac{\mathrm{f}}{8}\right) \cdot (\mathrm{Re_{air}} - 1000) \cdot \mathrm{Pr_{air}}}{1 + 12{,}7 \cdot \left(\frac{\mathrm{f}}{8}\right)^{\frac{1}{2}} \cdot (\mathrm{Pr_{air}}^{\frac{2}{3}} - 1)} \quad \text{(eq. 6)}$$

$$\mathrm{f} = (0{,}790 \cdot \ln(\mathrm{Re_{air}}) - 1{,}64)^{-2} \quad \text{(eq. 7)}$$

Using eq. 4 and eq. 6, the internal convective heat transfer coefficient can be calculated, resulting in all heat transfer coefficients of eq. 1 being identified as functions of various collector temperatures. Eq. 1 can now be used as one out of four equations of the equation system for the collector.

2.2.2 The air flow

Unlike the glazing, the air flowing through the collector will not absorb or emit any considerable amounts of heat radiation. The heat gains and losses of the air flow will thus only be convective heat transfer as well as the energy required to raise the temperature of the air. Since the air will contain moisture, especially in a sub-tropical country such as Mozambique, the water vapour passing through the collector should also be considered. Taking the water vapour into consideration will also be important for determining the drying rate.

The absorber and the inner sides of the collector will transfer heat to the air through convection, resulting in the first two terms of eq. 8, the energy balance of the air flow. At the same time, convective heat losses are likely to occur towards the glazing, resulting in the third term of eq. 8. Note that the absorber area and the glazing area are equally large. The fourth and fifth term of eq. 8 are representing the heat that is absorbed by the air flow, where the fourth term is dry air and the fifth term is water vapour.

$$\mathrm{h_{con,in}} \cdot \mathrm{A_{abs}} \cdot \left(\mathrm{T_{abs}} - \frac{\mathrm{T_{in}}+\mathrm{T_{out}}}{2}\right) + \mathrm{h_{con,in}} \cdot \mathrm{A_{sides}} \cdot \left(\frac{\mathrm{T_{abs}}+\mathrm{T_{glass}}}{2} - \frac{\mathrm{T_{in}}+\mathrm{T_{out}}}{2}\right) - \mathrm{h_{con,in}} \cdot \mathrm{A_{abs}} \cdot \left(\frac{\mathrm{T_{in}}+\mathrm{T_{out}}}{2} - \mathrm{T_{glass}}\right) - (\mathrm{T_{out}} - \mathrm{T_{in}}) \cdot \rho_{\mathrm{air}} \cdot \mathrm{C_{P,air}} \cdot \mathrm{u_{air}} \cdot \mathrm{A_{inlet}} - (\mathrm{T_{out}} - \mathrm{T_{in}}) \cdot \mathrm{C_{P,H2O}} \cdot \mathrm{m_h} = 0 \quad \text{(eq. 8)}$$

Using eq. 4-7, $h_{con,in}$ can be identified in eq. 8, resulting in the water mass flow m_h, being the only unknown parameter of eq. 8. The air velocity u_{air} is not considered as being temperature-dependent in the model and is set to a constant value. To determine the mass of water that passes through the collector each second, the relative humidity of the ambient air can be used. The relative humidity is defined as the ratio between the vapour pressure of the water and the saturation pressure of pure water at the same temperature (Alvarez H., 2006). This is shown in eq. 9.

$$\mathrm{RH} = 100 \cdot \frac{\mathrm{P_w}}{\mathrm{P_{ws}}} \quad \text{(eq. 9)}$$

To find the partial pressure of the water vapour, the saturation pressure needs to be calculated for a specific temperature. Using Antoine's equation, found below as eq. 10, the saturation pressure can be calculated where *A*, *B* and *C* are constants valid for a certain interval of temperatures (R.K.Sinnot, 2005).

$$\log(P_{ws}) = A - \frac{B}{T+C} \quad \text{(eq. 10)}$$

Combining eq. 9 and eq. 10 results in the partial pressure P_w being identified as a function of the air temperature. The water vapour in the air flowing through the collector can be assumed to be an ideal gas, meaning that the mass flow of water through the collector can be calculated according to eq. 11 (Atkins P. & de Paula J., 2002), resulting in all parameters of eq. 8 being identified as functions of various collector temperatures.

$$\mathrm{m_h} = \frac{\mathrm{P_w}}{\mathrm{R_V} \cdot \mathrm{T_{amb}}} \cdot \mathrm{A_{inlet}} \cdot \mathrm{u_{air}} \quad \text{(eq. 11)}$$

2.2.3 The absorber

The absorber plate contains one unique parameter, being the effective solar irradiation G_e. To calculate G_e, the optical properties of the glazing and the absorbers ability to absorb sunlight needs to be considered in terms of reflection, transmission and absorption. The resulting equation can be found in eq. 12. Note that expression contains no absorbance coefficient for the glazing, since the glazing is assumed to not absorb any sunlight.

$$G_e = \frac{G \cdot \tau_{glass} \cdot \alpha_{abs}}{1 - R_{abs} \cdot R_{glass}} \quad \text{(eq. 12)}$$

Having identified G_e, the full equation for the energy balance for the absorber is set up according to eq. 13. Note that the energy losses from the interior walls to the exterior walls of the collector have been included in the energy balance, where the interior walls are assumed to have the mean temperature of the absorber and the glazing.

$$\begin{aligned} &G - h_{con,in} \cdot \left(T_{abs} - \frac{T_{in}+T_{out}}{2}\right) - h_{rad,in} \cdot \left(T_{abs} - T_{glass}\right) - \frac{\lambda_{bottom}}{t_{bottom}} \cdot \\ &\left(T_{abs} - T_{wall}\right) - \frac{\lambda_{side}}{t_{side}} \cdot \frac{A_{sides}}{A_{abs}} \cdot \left(\frac{T_{abs}+T_{glass}}{2} - T_{wall}\right) - h_{con,in} \cdot \frac{A_{sides}}{A_{abs}} \cdot \\ &\left(\frac{T_{abs}+T_{glass}}{2} - \frac{T_{in}+T_{out}}{2}\right) = 0 \end{aligned} \quad \text{(eq. 13)}$$

The parameter $h_{con,in}$ is calculated using the same method as for the glazing and the parameter $h_{rad,in}$ is calculated using eq. 2.

2.2.4 The external walls of the collector

The external walls of the collector include the bottom and the sides of the collector. The amount of heat being transferred from the external walls to the ambience are important to acknowledge, since these will correspond to the amount of heat that is lost through the insulation. All heat gains to the exterior walls will be heat being conducted from the interior or the collector through the insulation layer, as shown in first two terms of eq. 14.

$$\begin{aligned} &\frac{\lambda_{bottom}}{t_{bottom}} \cdot \left(T_{abs} - T_{wall}\right) + \frac{\lambda_{side}}{t_{side}} \cdot \frac{A_{sides}}{A_{abs}} \cdot \left(\frac{T_{abs}+T_{glass}}{2} - T_{wall}\right) - h_{con,out} \cdot \\ &\frac{(A_{abs}+A_{sides})}{A_{abs}} \cdot \left(T_{wall} - T_{amb}\right) - h_{rad,out1} \cdot \left(T_{wall} - T_{amb}\right) - h_{rad,out1} \cdot \frac{A_{sides}}{2 \cdot A_{abs}} \cdot \\ &\left(T_{wall} - T_{amb}\right) - h_{rad,out2} \cdot \frac{A_{sides}}{2 \cdot A_{abs}} \cdot \left(T_{wall} - T_{sky}\right) = 0 \end{aligned} \quad \text{(eq. 14)}$$

The heat losses of the external walls will occur by convection affecting the sides and the bottom, but also by radiation. The sides have been assumed to radiate 50 % towards the atmosphere and 50 % to the ground and the bottom of the collector will radiate towards the ground. This can be seen in eq. 14 as the last three terms, where $h_{rad,out1}$ and $h_{rad,out2}$ are calculated according to eq. 15 and eq. 16 respectively. The ground is assumed to have the same temperature as the ambient air, T_{amb}.

$$h_{rad,out1} = \varepsilon_{wall} \cdot \sigma \cdot \frac{T_{wall}^4 - T_{amb}^4}{T_{wall} - T_{amb}} \quad \text{(eq. 15)}$$

$$h_{rad,out2} = \varepsilon_{wall} \cdot \sigma \cdot \frac{T_{wall}^4 - T_{sky}^4}{T_{wall} - T_{sky}} \quad \text{(eq. 16)}$$

After identifying equations for energy balances for the glazing, the air flow, the absorber and the external walls of the collector, an equation system for eq. 1, eq. 8, eq. 13 and eq. 14 can be set up and solved for T_{out}, T_{abs}, T_{glass} and T_{wall}. To create more accurate results, the equation system can be solved multiple times after dividing the collector into segments, also known as the finite element method. The segments are distributed over the length of the collector and the equation system is solved individually for each segment. The calculated outlet air temperature of the first segment can then be used as the input temperature for the air flow of the next segment. As an example, if a 1 m long collector is divided into two segments the first segment will include the first 0,5 m of the collector and show the mean temperatures for that length. The reason why more segments enhance the accuracy of the simulation is because the radiative heat transfer

coefficient will vary from segment to segment in a non-linear manner.
The number of segments that can be used are unlimited using Maple 2015, but a higher number of segments (a higher resolution) will result in a slower simulation speed. The resolution used to generate the results of the study was set to 250, which can be regarded as more than sufficient for solar collectors since they are generally rather short.

2.3 The dryer

Once the air has been heated up in the solar collector, it will enter the dryer containing the SAP-pouches. The dryer is modelled according to Fig. 4, where three surfaces can be identified; the dryer air flow, the internal- and the external walls of the dryer. Unlike the collector, the dryer will be split up in segments according to the number of shelves within the dryer, where each shelf will hold a certain number of SAP-pouches from which water will evaporate. Note that Fig. 4 is an example of a dryer section for a dryer holding one SAP-pouch per shelf. The released water from the shelves will accumulate from shelf to shelf, which will increase the resistance for evaporation of the bags further up in the dryer.

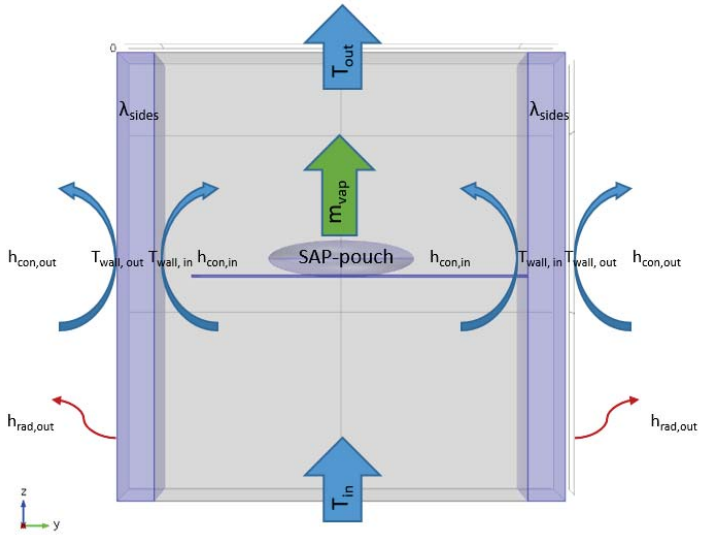

Fig. 4 : Schematic figure for all energy flows and temperatures that are included in the model for the dryer. Energy balances for the air flow, inner and outer wall of the collector will be set up according to this figure.

2.3.1 The internal walls of the dryer

The energy balance for the internal walls of the dryer include convective heat transfer from the dryer air flow as well as conductive heat transfer through the dryer insulation layer, shown in eq. 17.

$$h'_{con,in} \cdot \left(\frac{T_{in}+T_{out}}{2} - T_{wall,in}\right) - \frac{\lambda_{dryer}}{t_{side}} \cdot \left(T_{wall,in} - T_{wall,out}\right) = 0 \qquad \text{(eq. 17)}$$

Note that $h'_{con,in}$ is calculated using the same method as for the collector, but the air velocity in the dryer could differ from the collector. If the cross section area of the dryer is larger than the cross section area of the collector, the air velocity will be lower in the dryer than in the collector. A different air velocity and a different cross section will result in a new Reynold's number, meaning that the flow characteristics of the collector and the dryer could be different. For this reason, the Reynold's number for the dryer needs to be calculated.

2.3.2 The external walls of the dryer

The energy balance for the external sides of the dryer is set up according to the same method used for the collector sides in section 2.2.4, meaning that half of the heat radiation will radiate towards the ground and half will radiate towards the sky. The resulting equation can be found in eq. 18, in accordance with Fig. 4. One parameter that has been added to the energy balance for the external walls of the dryer is the additional heat gain z. The additional heat gain represents the average solar irradiation of all four outer walls of the dryer. The additional heat gains will increase the outer wall temperature of the dryer, which will reduce the heat losses through the walls or, if the outer walls are warmer than the inner walls, add heat to the air.

$$\frac{\lambda_{dryer}}{t_{side}} \cdot \left(T_{wall,in} - T_{wall,out}\right) - h_{con,out} \cdot \left(T_{wall,out} - T_{amb}\right) - \frac{1}{2} \cdot h_{rad,out1} \cdot \left(T_{wall,out} - T_{amb}\right) - \frac{1}{2} \cdot h_{rad,out2} \cdot \left(T_{wall,out} - T_{sky}\right) + z = 0 \quad \text{(eq. 18)}$$

2.3.3 The dryer air flow

For the dryer air flow, the same method used in section 2.2.2 for the collector air flow is used with the addition of a mass flux of water vapor from the SAP-pouches. This means that the calculations need to include an accumulation of the water molecules from shelf to shelf. For the first shelf, the inlet mass flux of water will be according to the absolute humidity which was calculated in the collector, m_h, while the outlet mass flux will also have gained water vapour from the SAP-pouches of the first shelf. The outlet mass flux of water from the first shelf will then be used as input for the inlet mass flux of water for the second shelf. Also note that the shelf is placed in the center of the dryer section, meaning that the SAP-pouch will have the section mean air temperature at steady state. The full expression used for the dryer air flow can be found in eq. 19, where E_{vap} corresponds to the amount of energy absorbed by the SAP-pouches, see eq. 20.

$$\left(T_{in} - T_{out}\right) \cdot \rho_{air} \cdot C_{P,air} \cdot u_{air} \cdot A_{inlet,dryer} - h'_{con,in} \cdot A_{sides} \cdot \left(\frac{T_{in}+T_{out}}{2} - T_{wall,in}\right) + \left(T_{in} - T_{out}\right) \cdot Cp_{H2O} \cdot m_h + \left(\frac{T_{in}+T_{out}}{2} - T_{out}\right) \cdot Cp_{H2O} \cdot m_{vap} - E_{vap} = 0 \quad \text{(eq. 19)}$$

$$E_{vap} = m_{vap} \cdot \Delta h_{vap,H2O} \quad \text{(eq. 20)}$$

Combining eq. 19 and eq. 20, the only unknown parameter is m_{vap}, which can be regarded as the drying rate of the SAP-pouches. For this reason, finding a good way to calculate m_{vap} is essential to evaluate the solar dryer performance. Since SAP-pouches can consist of various materials, the drying rate will differ depending on the pouch material (Phinney et al., 2015). For this study, measurements were provided from a separate study[1] where the drying rate of a specific type of SAP-pouch was measured for different temperatures, air flow rates and relative humidity. The data provided from the measurements were used to create a mathematical expression for the drying rate as a function of relative humidity and air velocity, shown in eq. 21.

$$m_{vap} = \frac{A_{bags}}{3600} \cdot \left(-1{,}0015 \cdot u_{bags} - 0{,}9565\right) \cdot RH + 0{,}3088 \cdot u_{bags} + 0{,}6297 \quad \text{(eq. 21)}$$

Note that the SAP-pouches will obstruct the air flow, reducing the effective cross section area of the dryer. To take this into consideration, the air velocity used to calculate the drying rate u_{bags} is calculated for the effective cross section area of the dryer. In other words, placing more SAP-pouches per shelf results in a higher u_{bags}.
The relative humidity *RH* of eq. 21 is calculated for the conditions around the SAP-pouches, i.e. the absolute humidity and the dryer air temperature.

3. Results

The main aim of the study was to create a calculation tool in Maple 2015 which can be used to generate approximate values for the drying rate and various temperatures for a user defined design of a solar dryer. Using the method described a calculation tool was built capable of simulating temperatures for the absorber, the glazing, the air flow and the external walls of the collector as well as the drying rate and temperatures of the air flow, internal- and external walls of the dryer. However, it was also decided to include a parametric study to find ways of improving the solar dryer performance. Several parameters were examined, where the most important ones will be presented in this paper with regards to temperature increase, drying rate how and suitable the solution would be to a developing country.

[1] Phinney, R. Unpublished data. Department of Food Technology, Engineering and Nutrition. Lund University

3.1 Adding fins to the absorber plate

To simulate fins being added to the absorber plate, a factor was added to the second term of eq. 13, being the convective heat transfer from the absorber plate to the air flow. As an example, a convective heat transfer factor of 2 means that fins with a total area equal to the absorber plate have been installed. A factor of 3 means that the area of the fins is twice as large as the collector plate and so on. The outlet air temperature of the collector, i.e. the inlet air temperature for the dryer, for various convective heat transfer factors can be found in Fig. 5. A schematic example of a collector with fins can be found in Fig. 7.

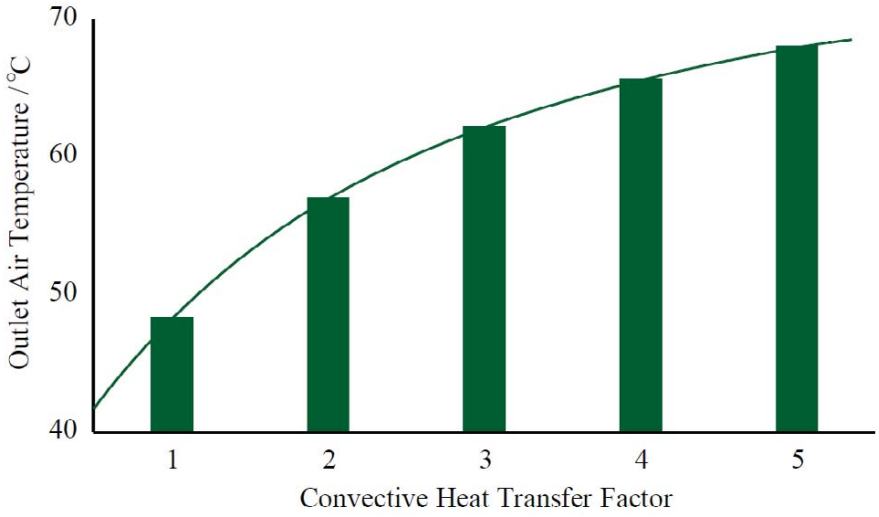

Fig. 5 : Calculated outlet temperatures of the collector for the base scenario for different convective heat transfer coefficient factors of the absorber.

3.2 Varying the number of SAP-pouches in the dryer

The number of SAP-pouches placed in the dryer is likely to affect the drying rate, since more bags per shelf will cause greater accumulation of water vapour from shelf to shelf. Varying the number of pouches placed per shelf is also a way of simulating the effects of uncertainties of the equation used for the drying rate, eq. 21. For the results of the study, simulations were made for 1, 2 and 3 pouches per shelf for a dryer with 8 shelves. The results for the drying rate per shelf can be found in Fig. 6.

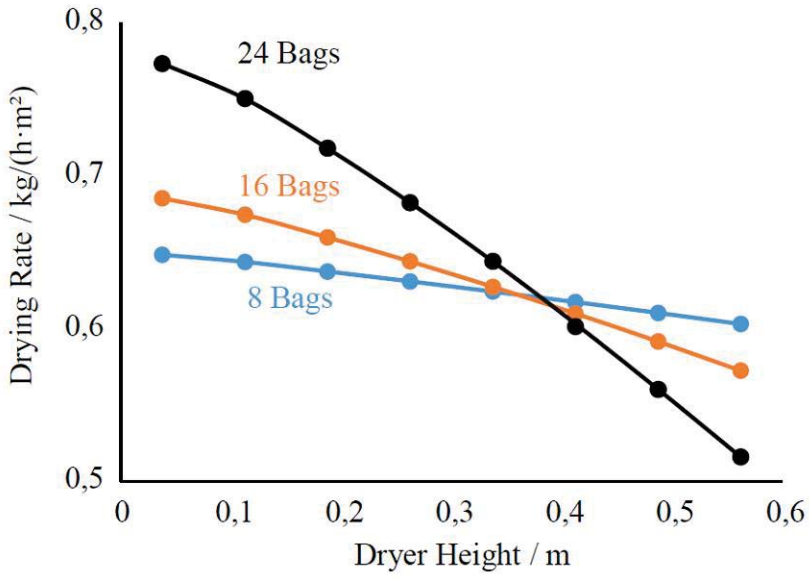

Fig. 6 : Simulated values for the drying rate for one (blue), two (orange) and three (back) SAP-pouches per shelf. Each dot represents one of the eight shelves inside the 0,6 m high dryer.

4. Discussion

4.1 Adding fins to the absorber

Increasing the outlet air temperature of the collector is a good method for increasing the drying rate. For the model used in this study, a higher air temperature results in a lower relative humidity inside the dryer, which increases the drying rate in eq. 21. Several different methods can be used to increase the air temperature of the collector, but it's important to consider which methods that are applicable in a developing country.

To avoid potential problems with complex materials unsuitable for developing countries, fins can be built using cheap materials with sufficient heat conductivity, see Fig. 7. The fins will conduct heat from the absorber, practically resulting in the contact area between the air flow and the absorber to be increased. As shown in Fig. 5, adding fins has good potential of increasing the collector air temperature and thus the drying rate. The air temperature gains from adding fins appears to decrease exponentially with increased convective heat transfer coefficients. This indicates that fins are most efficient for low convective heat transfer coefficients, as the temperature gains from adding excessive amounts of fins may not justify the material costs.

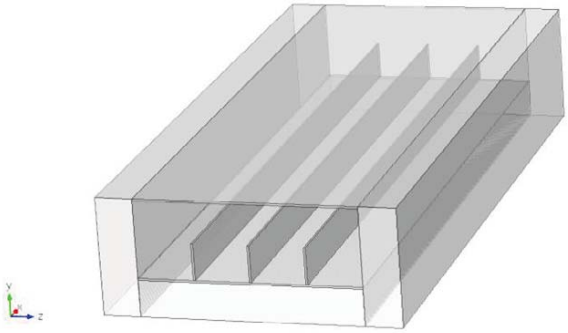

Fig. 7 : Schematic picture of a solar collector with fins attached to the absorber.

4.2 Potential problems with overloading the dryer

As shown in Fig. 6, the drying rate of the SAP-pouches will differ from the entrance to the outlet of the dryer. The pouches placed on the first shelf, closest to the entrance, will be exposed to a lower relative humidity than the pouches placed further up in the dryer. This occurs due the absolute humidity being higher further up in the dryer as well as the temperature being lower, since heat will be absorbed by the pouches and lost through the walls. Both the lower air temperature and the higher absolute humidity will result in a higher relative humidity, which reduces the drying rate. Also, if the SAP-pouches are obstructing a large portion of the dryer cross section area the air velocity surrounding the pouches will be higher, which according to the model will result in a higher drying rate. This can be seen in Fig. 6, where the drying rate for the first shelf is considerably higher when placing three pouches per shelf compared to placing one pouch per shelf.
Bearing the variations of the drying rate this in mind, it's important to acknowledge that every pouch placed in the dryer is required to have a sufficient drying rate. If the drying rate variation is too great, it could result in only the pouches placed on the first shelf to dry out completely. The lower drying rate of the remaining shelves could also cause the drying process to become too slow, resulting in the contents of the pouches becoming spoiled.

To avoid the problem described, there are two parameters worth considering; the volumetric air flow of the dryer and the number of SAP-pouches placed in the dryer. Increasing the volumetric air flow in the dryer results in better ventilation of the vapour generated by the pouches. To increase the volumetric air flow, the air velocity in the dryer could be increased. This will have two positive effects according to eq. 21, as the air velocity is increased and the relative humidity is decreased.
But increasing the volumetric air flow also has negative effects on the drying rate. Since the dryer is connected to the collector, the volumetric air flow will also be increased inside the collector. This will result in lower air temperatures in the collector and thus in the dryer.
Furthermore, increasing the air flow could require installations of fans. While fans are very likely to improve the solar dryer performance, they may not be a suitable solution in a developing country since a source of electricity is required. As a conclusion, finding a good balance between the collector outlet temperature, the dryer air velocity and the number of pouches placed in the dryer is the key to designing a good solar dryer.

5. References

Alvarez H. (2006). *Energiteknik.* Lund: Studentlitteratur AB.

Atkins P. & de Paula J. (2002). *Atkins' Physical Chemistry.* Oxford: Oxford University Press.

Blanco-Cano et al. (2016). Modeling the thin-layer drying process of Granny Smith apples: Application in an indirect solar dryer. *Applied Thermal Engineering Volume 108*, 1086–1094.

Department of Chemical Engineering of Lund University. (2013). *Handbook.* Lund: MediaTryck.

Incropera, F. P., & Dewitt, D. P. (2002). *Fundamentals of Heat and Mass Transfer.* New York: John Wiley & Sons, Inc.

Kumar et al. (2015). *Progress in solar dryers for drying various commodities.* Hisar, India: Guru Jambheshwar University of Science & Technology.

Kumar Moningi, M. (2016, March 29). *Conduction Convection Radiation processes of a solar collector using FEA*. Retrieved from unix.ecs.umass.edu: http://www-unix.ecs.umass.edu/mie/labs/mda/fea/fealib/moningi/moningiReport.pdf

Maplesoft. (2016, August 29). *New Maple 2016 offers advanced problem-solving for math, science, engineering*. Retrieved from Maplesoft: http://www.maplesoft.com/company/publications/articles/view.aspx?SID=154030

Mills-Gray, S. (1994, May 15). *Quality for Keeps: Drying Foods*. Retrieved from University of Missouri Extension: http://extension.missouri.edu/p/GH1562

PAEGC & TH Cologne. (2016). *Renewable Energy Resources and Technology Overview (Chapter B1)), Massive Open Online Course (MOOC).* Retrieved from Powering Agriculture - Sustainable Energy for Food: https://gc21.giz.de/ibt/var/app/wp385P/2624/wp-content/uploads/2015/03/PAEGC_MOOC_COMPILED_READER.pdf

Phinney et al. (2015). *Solar assisted pervaporation (SAP) for preserving and utilizing fruits in developing countries.* Kruger National Park, South Africa: Third Southern African Solar Energy Conference.

R.K.Sinnot. (2005). *Chemical Engineering Design: Chemical Engineering Volume 6.* Swansea: Butterworth-Heinemann.

Sekhar et al. (2009). Evaluation of Heat Loss Coefficients in Solar Flat Plate Collectors. *ARPN Journal of Engineering and Applied Sciences*, 15-19.

UNDP. (2015). *Briefing note for countries on the 2015 Human Development Report, Mozambique.* New York: UNDP.

World Food Programme. (2016, February 20). *Mozambique*. Retrieved from World Food Programme: http://www.wfp.org/countries/mozambique

6. Appendix

6.1. Nomenclature

A_{abs}	Collector absorber area (= glass area)	m²
A_{bag}	The effective area for evaporation of a SAP-pouch	m²
A_{bags}	Total effective evaporation area of SAP-pouches per shelf	m²
A_{eff}	Effective cross section area for the dryer airflow	m²
A_{inlet}	Collector inlet area	m²
A_{sides}	Collector side area	m²
a_w	Water activity	1
$C_{P,\ air}$	Specific heat capacity for air	J/(kg·K)
$C_{P,\ H2O}$	Specific heat capacity for steam	J/(kg·K)
D_H	Hydraulic diameter of the collector	m
E_{vap}	Total power required for evaporation for all SAP-pouches placed on a shelf in the dryer	W
G	Total solar irradiation	W/m²
G_e	Effective solar irradiation (heat absorbed by the absorber)	W/m²
$h_{con,\ in}$	Heat transfer coefficient for internal convection	W/(m²·K)
$h_{con,\ out}$	Heat transfer coefficient for external convection	W/(m²·K)
$h_{rad,\ in}$	Heat transfer coefficient for internal radiation	W/(m²·K)

$h_{rad,\ out}$	Heat transfer coefficient for external radiation	W/(m²·K)
m_h	Water mass flow	kg/s
m_{vap}	Water mass flow from SAP-pouch	kg/s
n	Number of bags per shelf in the dryer	1
Nu	Nusselt number for uniform surface heat flux	1
Pr_{air}	Prandtl number for air	1
P_w	Vapour pressure for water	Pa
P_{ws}	Water saturation pressure	Pa
R_{abs}	Absorber reflectance	1
Re_{air}	Reynolds number for air	1
R_{glass}	Glass reflectance	1
RH	Relative humidity	1
R_V	Specific gas constant for water vapour	J/(kg·K)
S	Number of shelves in the dryer	1
T_{abs}	Absorber temperature in the collector	K
T_{air}	Mean temperature of T_{in} and T_{out}	K
T_{amb}	Ambient temperature (= 25 °C for the simulations)	K
t_{bottom}	Bottom insulation thickness	m
T_{glass}	Glass temperature in collector	K
T_{in}	Inlet temperature for a section	K
T_{out}	Outlet temperature for a section	K
t_{side}	Side insulation thickness	m
T_{sky}	Sky temperature (= 5 °C for the simulations)	K
T_{wall}	Wall temperature of dryer	K
T_{wall}	Outer wall temperature in the collector	K
$T_{wall,\ in}$	Inner wall temperature in the dryer	K
$T_{wall,\ out}$	Outer wall temperature in the dryer	K
u_{air}	Collector inlet air velocity	m/s
u_{bags}	The air velocity surrounding the SAP-pouches	m/s
z	Additional heat gains for the outer walls of the dryer	W/m²
α_{abs}	Absorber absorbance	1
$\Delta h_{vap,\ H2O}$	Enthalpy of vaporization for water	J/kg
ε_{abs}	Absorber emissivity	1
ε_{glass}	Glass emissivity	1
ε_{wall}	Collector outer wall emissivity	1
$\varepsilon_{wall,\ dryer}$	Dryer outer wall emissivity	1
λ_{air}	Air thermal conductivity	W/(m·K)
λ_{bottom}	Collector bottom insulation thermal conductivity	W/(m·K)
λ_{side}	Collector side insulation thermal conductivity	W/(m·K)
λ_{wall}	Dryer wall thermal conductivity	W/(m·K)
μ_{air}	Air dynamic viscosity	kg/(m·s)
ρ_{air}	Air density	kg/m³
σ	Stefan-Boltzmann constant	W/ (m²·K⁴)
τ_{glass}	Glass transmissivity	1